

## QM/MM Studies of Monozinc $\beta$ -Lactamase CphA Suggest That the Crystal Structure of an Enzyme–Intermediate Complex Represents a Minor Pathway

Shanshan Wu,<sup>†</sup> Dingguo Xu,<sup>\*,†</sup> and Hua Guo<sup>\*,‡</sup>

MOE Key Laboratory of Green Chemistry and Technology, College of Chemistry, Sichuan University, Chengdu, Sichuan 610064, P. R. China, and Department of Chemistry and Chemical Biology, University of New Mexico, Albuquerque, New Mexico 87131, United States

Received May 17, 2010; E-mail: dgxu@scu.edu.cn; hguo@unm.edu

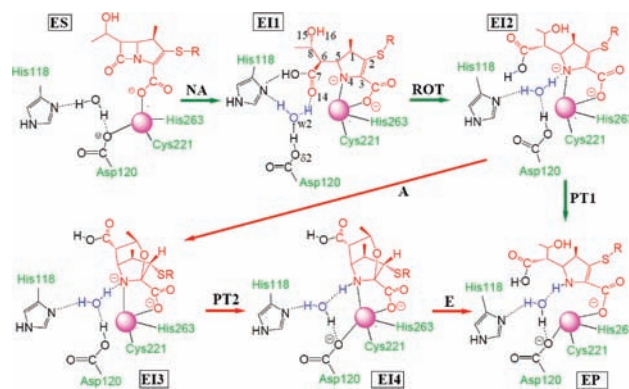
**Abstract:** QM/MM studies of the hydrolysis of a  $\beta$ -lactam antibiotic molecule (biapenem) catalyzed by a monozinc  $\beta$ -lactamase (CphA) have revealed the complete reaction mechanism and shown that an experimentally determined enzyme–intermediate complex is a stable intermediate or product in a minor pathway.

Bacterial resistance to  $\beta$ -lactam antibiotics such as penicillin, cephalosporins, and carbapenems is conferred by  $\beta$ -lactamases, which deactivate the antibiotic by hydrolyzing the common  $\beta$ -lactam ring.<sup>1,2</sup> While the mechanism of serine-based  $\beta$ -lactamases is well-established,<sup>2</sup> the mode of catalysis for metallo- $\beta$ -lactamases (M $\beta$ LS) is still not completely resolved.<sup>3,4</sup> The rapid proliferation of M $\beta$ LS genes from innocuous species to pathogenic ones via plasmid and/or integron-borne pathways, combined with the lack of clinically useful inhibitors, renders M $\beta$ LS a more potent threat than their serine-based counterparts.<sup>5,6</sup> Our incomplete understanding of the M $\beta$ LS catalytic mechanism hampers the search for effective inhibitors.

Mechanistic insights can often be gained from X-ray structures of an enzyme and perhaps more importantly its complexes with substrate analogues. This is no exception for M $\beta$ LS, where recently determined complex structures have shed valuable light on substrate binding modes and reaction pathways.<sup>7–9</sup> However, the very existence of an enzyme complex underscores its thermodynamic and/or kinetic stability. In other words, structures determined by X-ray crystallography are associated with wells on the free-energy landscape that may or may not be associated with the kinetically favored reaction pathways. In this communication, we argue on the basis of reliable quantum-mechanical/molecular-mechanical (QM/MM) calculations<sup>10–13</sup> that a recently determined X-ray structure of a monozinc M $\beta$ LS (CphA from the opportunistic pathogen *Aeromonas hydrophila*)<sup>7</sup> represents a stable intermediate or a product in a minor pathway for the hydrolysis of a carbapenem antibiotic molecule (biapenem).

Our QM/MM simulations were based on a recently determined X-ray structure of CphA complexed with a hydrolysis intermediate of biapenem,<sup>7</sup> hereafter denoted as the EI complex. As demonstrated in our earlier work,<sup>14,15</sup> the putative mechanism of CphA (Scheme 1) uses a non-zinc-bound water molecule as the nucleophile. In the initial nucleophilic addition (NA) step, the water nucleophile is assisted by the Asp120 general base to attack the carbonyl carbon of the substrate, leading to cleavage of the C<sub>7</sub>–N<sub>4</sub> bond in the lactam ring. The resulting anionic nitrogen is stabilized by the Zn(II) ion, forming an enzyme–intermediate complex. In the meantime, the zinc ion disengages the protonated Asp120 to maintain its tetrahedral coordination.

**Scheme 1.** Proposed Mechanism for the Hydrolysis of Biapenem Catalyzed by CphA; Two Pathways Are Depicted for the Second Step of the Hydrolysis, and the Purple Balls Represent the Zinc Ion



We report here the simulation of the complete catalysis mechanism for CphA. The details of our simulation methods are given in the Supporting Information (SI). Briefly, the self-consistent charge–density functional tight binding (SCC–DFTB) method<sup>16,17</sup> was used for the QM region while the surrounding MM region was described by the CHARMM all-atom force field.<sup>18</sup> The SCC–DFTB/MM method was extensively validated for this system by comparison with B3LYP/MM single-point calculations, as described in the SI. All of the simulations were carried out using CHARMM.<sup>19</sup>

Our simulations started by adding a H<sub>2</sub>O molecule in the active site, which hydrogen bonds with both the protonated Asp120 and His118 (see structure EI1 in Scheme 1). This was justified by the X-ray structure of the EI complex,<sup>7</sup> which has a H<sub>2</sub>O molecule in the same position. The reaction proceeds with a rotation around the C<sub>5</sub>–C<sub>6</sub> bond (ROT), as suggested by the X-ray structure.<sup>7</sup> The resulting structure EI2 provides the branching point for two pathways.

Pathway I completes the reaction by transferring a proton from Asp120 to the zinc-bound nitrogen via the water bridge (PT1). As shown in Figure 1, the barriers for both the ROT and PT1 steps are much lower than that for the NA step (14.1 kcal/mol).<sup>15</sup> The overall barrier for pathway I is consistent with kinetic data on this<sup>7</sup> and similar M $\beta$ LS,<sup>20</sup> and I represents the kinetically favored pathway.

However, it is clear that pathway I cannot explain the existence of the experimentally observed EI complex,<sup>7</sup> which features an additional ring structure formed by addition of the hydroxyl group at the C<sub>8</sub> position to the C<sub>2</sub>=C<sub>3</sub> double bond. To reach the experimental structure, we computed the free-energy profile for a second pathway (II) that starts with the addition (A) reaction, which

<sup>†</sup> Sichuan University.

<sup>‡</sup> University of New Mexico.

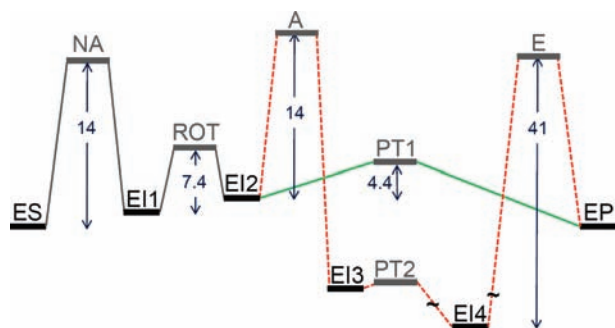


**Figure 1.** Free-energy profiles of the catalytic reaction. The two pathways are represented by green (I) and red (II) lines. Only forward barriers (in kcal/mol) are given.

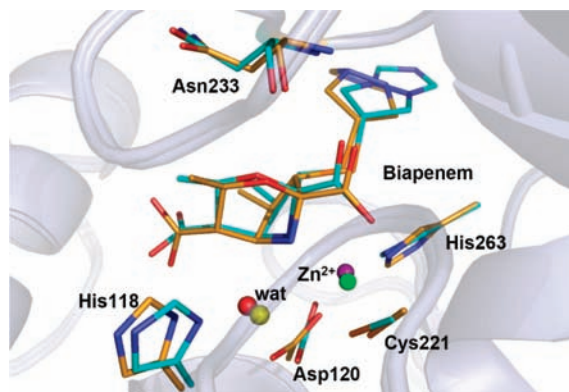


**Figure 2.** Overlap of active-site moieties between the calculated EI4 complex (cyan for the carbon atom, red for water, purple for the zinc ion) and the X-ray structure of the EI complex (orange for the carbon atoms, yellow for water, green for the zinc ion).<sup>7</sup> All hydrogen atoms are removed.

converts EI2 to EI3, as shown in Scheme 1. This is followed by the water-bridged proton transfer from the protonated Asp120 to the zinc-bound nitrogen (PT2), which is essentially barrierless, as shown in Figure 1. The resulting complex EI4 is structurally identical to the experimental EI complex. Specifically, the protonated N<sub>4</sub> atom is  $2.18 \pm 0.16$  Å away from the zinc ion, which compares favorably with the experimental value of  $2.22$  Å<sup>7</sup> but is quite different from the value in either EI1 ( $1.99 \pm 0.11$  Å) or EP ( $2.93 \pm 0.33$  Å). In Figure 2, the crystal structure is compared with a snapshot of the EI4 complex, and the overlap is quite satisfactory. A detailed comparison of the geometric parameters can be found in the SI.

As shown in Figure 1, the EI4 complex resides in a deep free-energy well in pathway II that is flanked by large barriers to EI3 and EP. It is clear that pathway II is kinetically uncompetitive with pathway I, but the thermodynamic stability of EI4 provides a conceivable explanation for its entrapment and observation in the X-ray diffraction experiment.<sup>7</sup> Interestingly, the CphA enzyme is inhibited by its product,<sup>7</sup> which might very well be the stable double-ring structure in EI4 because of the high barrier to EP.

It should be pointed out that there are other mechanistic proposals for CphA catalysis. Specifically, Simona et al.<sup>21</sup> have recently advanced a mechanism with concerted NA and PT steps. However, this mechanism was based on an initial ES configuration in which the substrate binds indirectly with zinc through a water molecule. This model is thus inconsistent with a large body of experimental data suggesting a direct substrate–zinc contact through the functionally conserved carboxylate of  $\beta$ -lactam antibiotics.<sup>4</sup> These data include X-ray absorption<sup>22</sup> and electron paramagnetic resonance (EPR)<sup>23</sup> spectra as well as X-ray

structures of M $\beta$ Ls complexed with various substrate analogues.<sup>7–9</sup> The mechanism proposed by Simona et al. also precludes the existence of an anionic nitrogen intermediate,<sup>24–28</sup> which is considered as a common determinant in M $\beta$ L catalysis.<sup>3</sup> In particular, such an intermediate has recently been observed in a monozinc M $\beta$ L (GOB) with a very similar active-site arrangement.<sup>29</sup> In contrast, the mechanism outlined in Scheme 1 is consistent with all of the known experimental observations and earlier theoretical studies.<sup>30,31</sup>

The demonstration that the crystal structure of EI represents a stable intermediate/product in a minor pathway in CphA catalysis is probably not an isolated case. Numerous examples can be found where crystal structures depict nonproductive configurations for binding and reaction. Thus, sole reliance on X-ray structures could lead to incorrect or incomplete mechanisms. However, we also want to emphasize that it is not our intention to discount the paramount importance of crystal structures in elucidating catalytic mechanisms. Indeed, the proposed mechanism owes its existence largely to the X-ray structure of CphA. However, caution must be exercised in such endeavors. To this end, reliable theoretical models will play an increasingly indispensable role in checking the viability of various mechanistic proposals.

To summarize, detailed QM/MM free-energy simulations have allowed us to map out the entire reaction pathway for the hydrolysis of a carbapenem antibiotic molecule catalyzed by a monozinc M $\beta$ L. In addition, it has been demonstrated that the experimentally observed enzyme–intermediate complex is involved in a minor pathway.

**Acknowledgment.** This work was funded by the SRF for ROCS, SEM (20091001-9-7), and the Natural Science Foundation of China (20803048 and 21073125) to D.X. and by the National Institutes of Health (R03-AI071992) to H.G. Parts of the calculations were carried out at the National Center for Supercomputing Applications.

**Supporting Information Available:** Details about the methods used in this work, additional results, and complete ref 18. This material is available free of charge via the Internet at <http://pubs.acs.org>.

## References

- Walsh, C. *Nature* **2000**, *406*, 775.
- Fisher, J. F.; Meroueh, S. O.; Mobashery, S. *Chem. Rev.* **2005**, *105*, 395.
- Wang, Z.; Fast, W.; Valentine, A. M.; Benkovic, S. J. *Curr. Opin. Chem. Biol.* **1999**, *3*, 614.
- Crowder, M. W.; Spencer, J.; Vila, A. J. *Acc. Chem. Res.* **2006**, *45*, 13650.
- Walsh, T. R.; Toleman, M. A.; Poirel, L.; Nordmann, P. *Clin. Microbiol. Rev.* **2005**, *18*, 306.
- Oelschlaeger, P.; Ai, N.; DuPrez, K. T.; Welsh, W. J.; Toney, J. H. *J. Med. Chem.* **2010**, *53*, 3013.
- Garau, G.; Bebrone, C.; Anne, C.; Galleni, M.; Frere, J.-M.; Dideberg, O. *J. Mol. Biol.* **2005**, *345*, 785.
- Spencer, J.; Read, J.; Sessions, R. B.; Howell, S.; Blackburn, G. M.; Gamblin, S. J. *J. Am. Chem. Soc.* **2005**, *127*, 14439.
- Lienard, M. N. R.; Garau, G.; Horsfall, L.; Karsisotis, A. I.; Damblon, C.; Lassaux, P.; Papamicael, C.; Roberts, G. C. K.; Galleni, M.; Dideberg, O.; Frere, J.-M.; Schofield, C. J. *Org. Biomol. Chem.* **2008**, *8*, 2282.
- Warshel, A.; Levitt, M. J. *Mol. Biol.* **1976**, *103*, 227.
- Gao, J. *Acc. Chem. Res.* **1996**, *29*, 298.
- Riccardi, D.; Schaefer, P.; Yang, Y.; Yu, H.; Ghosh, N.; Prat-Resina, X.; König, P.; Li, G.; Xu, D.; Guo, H.; Elstener, M.; Cui, Q. *J. Phys. Chem. B* **2006**, *110*, 6458.
- Senn, H. M.; Thiel, W. *Angew. Chem., Int. Ed.* **2009**, *48*, 1198.
- Xu, D.; Zhou, Y.; Xie, D.; Guo, H. *J. Med. Chem.* **2005**, *48*, 6679.
- Xu, D.; Xie, D.; Guo, H. *J. Biol. Chem.* **2006**, *281*, 8740.
- Elstner, M.; Porezag, D.; Jungnickel, G.; Elsner, J.; Haugk, M.; Frauenheim, T.; Suhai, S.; Seigert, G. *Phys. Rev. B* **1998**, *58*, 7260.
- Cui, Q.; Elstner, M.; Kaxiras, E.; Frauenheim, T.; Karplus, M. *J. Phys. Chem. B* **2001**, *105*, 569.
- MacKerell, A. D., Jr.; et al. *J. Phys. Chem. B* **1998**, *102*, 3586.
- Brooks, B. R.; Brucoleri, R. E.; Olafson, B. D.; States, D. J.; Swaminathan, S.; Karplus, M. *J. Comput. Chem.* **1983**, *4*, 187.
- Sharma, N. P.; Hajdin, C.; Chandrasekar, S.; Bennett, B.; Yang, K.-W.; Crowder, M. W. *Biochemistry* **2006**, *45*, 10729.

- (21) Simona, F.; Magistrato, A.; Dal Peraro, M.; Cavalli, A.; Vila, A. J.; Carloni, P. *J. Biol. Chem.* **2009**, *284*, 28164.
- (22) Costello, A. L.; Sharma, N. P.; Yang, K.-W.; Crowder, M. W.; Tierney, D. L. *Biochemistry* **2006**, *45*, 13650.
- (23) Garrity, J. D.; Bennett, B.; Crowder, M. W. *Biochemistry* **2005**, *44*, 1078.
- (24) Wang, Z.; Fast, W.; Benkovic, S. J. *Biochemistry* **1999**, *38*, 10013.
- (25) McManus-Munoz, S.; Crowder, M. W. *Biochemistry* **1999**, *38*, 1547.
- (26) Hu, Z.; Periyannan, G.; Bennett, B.; Crowder, M. W. *J. Am. Chem. Soc.* **2008**, *130*, 14207.
- (27) Tioni, M. F.; Llarrull, L. I.; Poeylout-Palena, A. A.; Marti, M. A.; Saggi, M.; Periyannan, G.; Mata, E. G.; Bennett, B.; Murgida, D. H.; Vila, A. J. *J. Am. Chem. Soc.* **2008**, *130*, 15852.
- (28) Tomatis, P. E.; Fabiane, S. M.; Simona, F.; Carloni, P.; Sutton, B. J.; Vila, A. J. *Proc. Natl. Acad. Sci. U.S.A.* **2008**, *105*, 20605.
- (29) Lisa, M.-N.; Hemmingsen, L.; Vila, A. J. *J. Biol. Chem.* **2010**, *285*, 4570.
- (30) Park, H.; Brothers, E. N.; Merz, K. M., Jr. *J. Am. Chem. Soc.* **2005**, *127*, 4232.
- (31) Xu, D.; Guo, H.; Cui, Q. *J. Am. Chem. Soc.* **2007**, *129*, 10814.

JA104241G